

# A discrete model of filtrational gas combustion

Fedir Sirotkin, Roman Fursenko, Sergey Minaev  
Far Eastern Federal University  
Vladivostok, Russia

## 1 Introduction

Filtration gas combustion in a porous media has attracted considerable interest due to a large number of applications such as lean mixtures burning, reduction of pollutants emission, methane to hydrogen conversion, power engineering, etc., [1, 2]. Heat feed-back from the high temperature combustion products by radiation and conduction through solid medium serves to preheat incoming mixture [3]. This heat recirculation mechanism leads to several features, namely higher burning velocities, superadiabatic temperature in the reaction zone [4, 5], extension of the flammability limits [6, 7], low emission of pollutants [8], and the ability to burn low-caloric fuels.

In a recent past, various 1D and 2D continuous models have been developed and applied to filtration gas combustion problem. Although these models are good for predictions of the flame thickness, filtrational combustions speed and temperature distribution [1, 9], a fragmentation of the flame front and other effects related to the discrete structure of the porous media are beyond the scope of the continuous formulation. Unfortunately, the complete 3D modeling of filtrational gas combustion has a high complexity due to high computational load.

We propose the compromise 2D model of filtrational gas combustion which utilizes thermal-diffusion approach and takes into account the discrete structure of the porous media. Our method consists of three steps. On the first step, the porous media of the given porosity is generated by randomly placing solid grains. On the second step, the velocity field is calculated. On the last step, the thermal-diffusion model is applied to calculate the flame propagation.

## 2 Mathematical model

The porous media is generated by randomly placing solid grains on the uniform rectangular mesh. The grain's size varies randomly within  $[d_{\max}, d_{\min}]$  range. The porosity is defined as  $\epsilon = 1 - S_s/S_t$ , where  $S_t$  and  $S_s$  are the total area of the porous media and the area of solid grains. The flow structure is computed using Smoothed Particle Hydrodynamics method (SPH).

Flame propagation in the porous media is described via thermal-diffusion model using the flow field obtained on the previous step. Within the framework of this model the one-step irreversible Arrhenius type exothermic chemical reaction is applied. The gas density, thermal and molecular diffusion coefficients are assumed to be constants. The set of equations for the gaseous phase can be written as:

$$\rho_g c_{pg} \left( \frac{\partial T_g}{\partial t} + \mathbf{u} \cdot \nabla T_g \right) = \lambda_g \Delta T_g + \rho_g Q R(Y_F, T_g), \quad (1)$$

$$\frac{\partial Y_F}{\partial t} + \mathbf{u} \cdot \nabla Y_F = D_m \Delta Y_F - R(Y_F, T_g), \quad (2)$$

where  $T_g$  is the temperature of the gas,  $\mathbf{u}$  is the velocity vector,  $Y_F$  is the fuel mass fraction,  $\rho_g$  is the gas density,  $c_{pg}$  is the gas heat capacity,  $\lambda_g$  is the heat conductivity, and  $D_m$  is the molecular diffusion coefficient. The chemical reaction rate is defined as:

$$R(Y_F, T_g) = k Y_F \exp(-T_a/T_g), \quad (3)$$

where  $T_a$  is the activation temperature. Using of the single step chemical kinetics is justified because the detailed chemistry is important only for rich and near stoichiometric mixtures [1, 10].

In order to include the conductive heat transfer through the solid phase in the frame of two-dimensional model, the porous media is modeled as a set of cylindrical elements which are placed between solid plates. The average height and diameter of cylinders are equal. The plate's thickness is equal to the average diameter of solid grains,  $\bar{d}$ . For such geometrical design 3D equations for the solid phase can be reduced to 2D case and written as:

$$\rho_s c_s \frac{\partial T_s}{\partial t} = \lambda_s \Delta T_s + \frac{\lambda_s}{\bar{d}^2} (T_p - T_s), \quad (4)$$

$$\rho_s c_s \frac{\partial T_p}{\partial t} = \lambda_s \Delta T_p - g(x, y) \frac{\lambda_s}{\bar{d}^2 (1 - \epsilon)} (T_p - T_s), \quad (5)$$

where  $c_s$  is the heat capacity of the solid,  $\lambda_s$  is the heat conductivity.  $T_s$  is the temperature of the solid phase,  $T_p$  is the temperature of the artificial plate. The function  $g$  is introduced in order to account the heat transfer only in the areas of the contact between the solid grains and the artificial plate:

$$g(x, y) = \begin{cases} 1, & \text{if } (x, y) \in \text{solid grains,} \\ 0, & \text{if } (x, y) \in \text{gaseous phase.} \end{cases} \quad (6)$$

Equations (1)-(5) are solved in the rectangular domain  $0 \leq x \leq L_x$ ,  $0 \leq y \leq L_y$ . The boundary conditions at the inlet are

$$Y_F = Y_0, \quad T_s = T_g = T_p = T_0, \quad (7)$$

where  $T_0$  is the temperature and  $Y_0$  is the fuel mass fraction of the unreacted mixture. The boundary conditions at the outlet are

$$\frac{\partial Y_F}{\partial x} = 0, \quad \frac{\partial T_s}{\partial x} = 0, \quad \frac{\partial T_g}{\partial x} = 0, \quad \frac{\partial T_p}{\partial x} = 0. \quad (8)$$

The periodic boundary conditions at  $y = 0$  and  $y = L_y$  are applied. The boundary conditions at the interface between solid grains and the gaseous phases are:

$$\frac{\partial Y_F}{\partial \mathbf{n}} = 0, \quad \frac{\partial T_g}{\partial \mathbf{n}} = \frac{\alpha}{\lambda_g} (T_g - T_s), \quad \frac{\partial T_s}{\partial \mathbf{n}} = \frac{\alpha}{\lambda_s} (T_g - T_s), \quad (9)$$

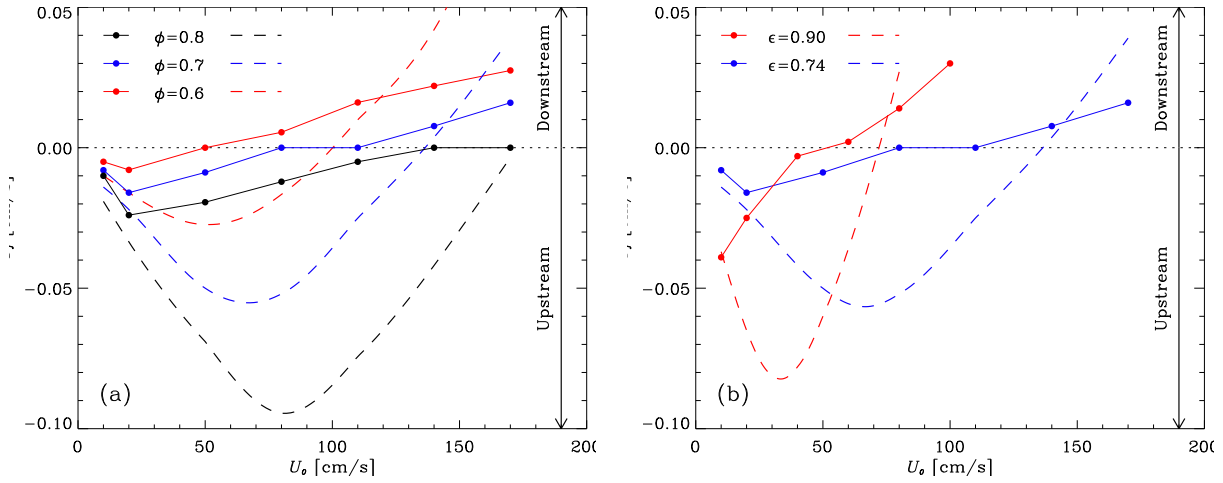


Figure 1: Dependencies of combustion wave propagation velocity  $U_f$  on the inlet velocity  $U_0$ .

where  $\alpha$  is the heat exchange coefficient,  $\mathbf{n}$  is the unit normal vector.

The set of equations (1)-(5) with boundary conditions (7)-(9) was solved numerically using explicit finite-difference scheme. The following parameters which roughly corresponds to combustion of methane-air mixture in the quartz porous media were utilized:  $\rho_s = 2.65 \cdot 10^3 \text{ kg/m}^3$ ,  $c_s = 0.84 \text{ kJ/kg} \cdot \text{K}$ ,  $\lambda_s = 8.0 \text{ W/m} \cdot \text{K}$ ,  $\rho_g = 1.2 \text{ kg/m}^3$ ,  $c_{pg} = 1.01 \text{ kJ/kg} \cdot \text{K}$ ,  $\lambda_g = 0.052 \text{ W/m} \cdot \text{K}$ ,  $Q/c_{pg} = 35000 \text{ K}$ ,  $k = 1.5 \cdot 10^8 \text{ s}^{-1}$ ,  $D_m \lambda_g / (\rho_g c_{pg}) = Le = 0.9$ ,  $\bar{d} = 3 \cdot 10^{-5} \text{ m}$ ,  $\alpha = 30 \text{ W/m}^2 \cdot \text{K}$ ,  $T_a = 15000 \text{ K}$ . The size of the porous media is  $2 \times 4 \text{ cm}$ . Convergence of the numerical solution was tested on the set of successively refining grids. For the spatial resolution better than 192 nodes per 1cm, the quantitative difference in the flame propagation velocity is less than 5%.

### 3 Results

Dependencies of combustion wave propagation velocity,  $U_f$ , versus inlet gas velocity,  $U_0$ , for different equivalence ratios is calculated on the basis of numerical solution as:

$$U_f = \frac{\Delta x_f}{\Delta t}, \quad x_f = \frac{\iint Y_F dx dy}{Y_0 L_y}.$$

Figure 1.a illustrates dependencies of combustion wave propagation velocity  $U_f$  on the inlet velocity  $U_0$  for different equivalence ratios. The porosity is  $\epsilon = 0.74$ , for the all illustrated cases. Solid lines with solid circles denote numerical results. Dashed lines illustrate numerical results obtained with the continuous two-temperature model for the same parameters.

The dependencies of  $U_f$  versus  $U_0$  have a U-shape which is typical for the low-velocity combustion regime [6, 11, 12]. We distinguish three main combustion regimes for the given porosity and equivalence ratio: upstream regime ( $U_f < 0$ ), downstream regime ( $U_f > 0$ ), and the flame anchoring regime ( $U_f \approx 0$ ).

The dependencies of flame propagation velocity on inlet gas velocity calculated for different porosities are shown in Figure 1.b. The average size of solid grains is the same in all cases. Qualitative behavior of these

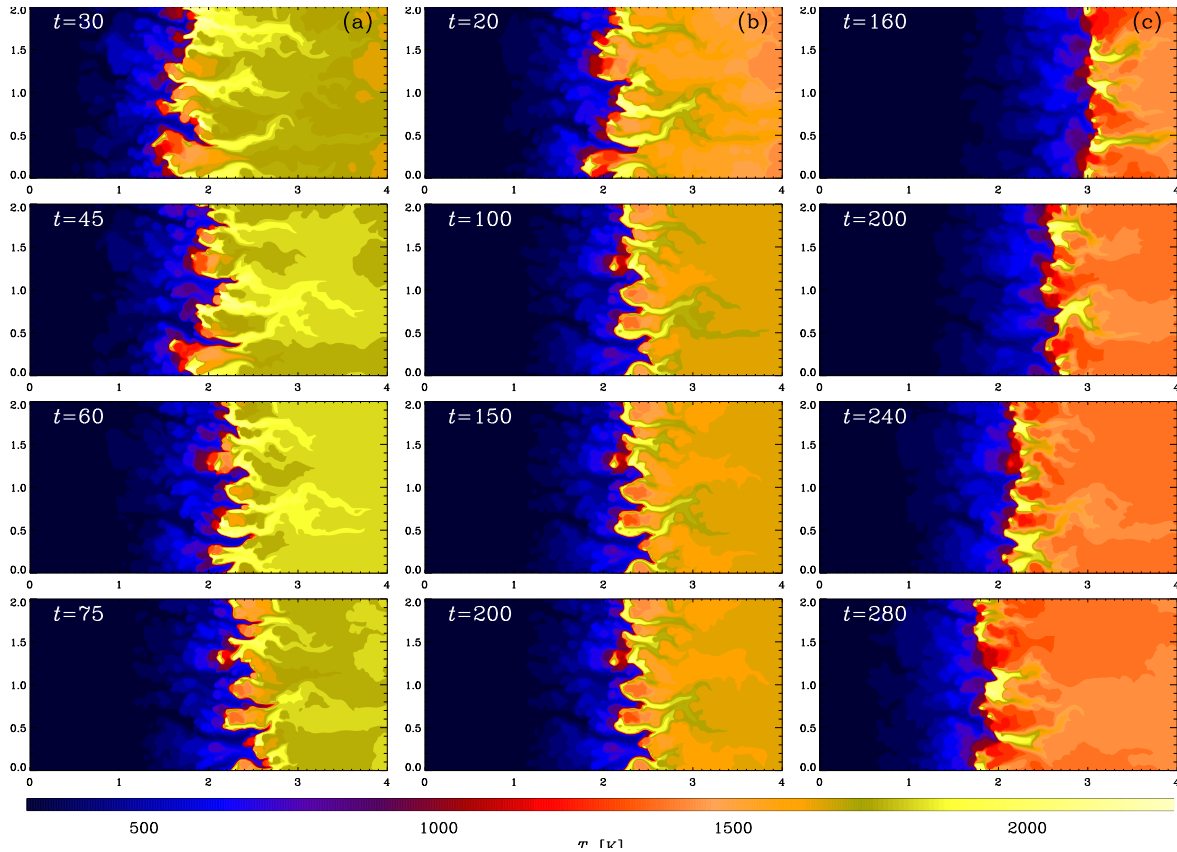


Figure 2: Temperature distribution in upstream (a), flame anchoring (b) and downstream (c) regimes.

dependencies versus conventional 1D continuous thermal-diffusion model (dashed lines) is the same. When the porosity increases, the overall thermal interaction between gas and solid phases reduces, leading to a more dramatic response of flame propagation velocity on variations of inlet velocity. For the limiting case when the porosity tends to unit, the preheating of the unburned mixture caused by the heat transfer within the gaseous phase as it happens for the freely propagating laminar flames.

Figure 2 illustrates the temperature distribution in these regimes when  $\phi = 0.7$  and  $\epsilon = 0.74$ . In the upstream regime the flame propagation is unsteady. The flame front consists of pulsating and stationary propagating regions. The location of these regions depends on the spatial distribution of solid grains. If the normal velocity of the flame front is close to the local gas velocity, the position of the flame front is quasi-stationary, otherwise the flame front fragment propagates upstream or downstream. When the local flame front reaches the region where the temperature of the porous media is low, the flame is quenching. After that the fresh mixture moves downstream and fills the area passed by the flame. Once the fresh mixture reaches the solid with high temperature the mixture is ignited again. This oscillating process repeats until the moment when the temperature of the porous media in the upstream direction is increased due to the heat exchange between the solid and gaseous phases. The amplitude of these pulsations is of the order of  $\bar{d}$  and decreases when the inlet velocity increases. The dynamical behavior of the local flame fronts resembles the flame repetitive ignition and extinction (FREI) phenomena [13].

When the inlet velocity increases, the combustion wave speed become close to zero within the some range of the  $U_0$  (see Figure 1.a). Figure 2.b illustrates numerical results for the flame anchoring regime. In this regime the combustion wave does not advance in the space and does not have oscillating parts, while the inlet velocity changes within a some range. The conventional two-temperature continuous model predicts that the flame front can be spatially stabilized only for a certain value of the filtration velocity. The flame anchoring effect was found in experimental investigations of filtration combustion in porous media made of micro-fibers [11]. Our numerical results and experimental data exhibit the same flame anchoring effect. A qualitative comparison demonstrates the capability of the proposed model to describe effects which can not be captured in the frame of continuous models.

Further increase of gas filtration velocity results in the downstream propagation of the flame. The flame wave propagation is quasi-uniform and does not accompanied with pulsation of separate hot spots which was observed in the range of small filtration velocities. The flame front is much more distorted when compared with upstream regime. The finger-like high temperature regions behind the flame front are formed in the course of flame propagation. These regions are located along the streamlines with high velocity magnitude. Because of high gas velocity in these streamlines, combustion products pass a relatively long distance before cooling to equilibrium temperature due to heat loss to the porous media. The increasing of the flame front area results in a higher total heat release when compared with that predicted by continuous model.

### 3 Conclusion

Due to the geometric complexity and numerous processes that have to be considered, filtration combustion is a very complicated process to investigate computationally. Conventional continuous model does not take into account many physical factors such as flow in a complex geometry, radiative heat transfer, fluid-solid interaction etc., and does not allow to predict some physical phenomena. Proposed numerical method makes possible to study impact of the discrete structure of the porous media on flame characteristics. In order to distinguish and highlight the impact of discrete structure, we made assumptions which are similar to those adopted in continuous thermal-diffusion model namely: the viscosity, radiative heat transfer effects and gas thermal expansion are neglected, the flow is decoupled from combustion via the thermo-diffusive approximation.

Our results imply that the flame propagation in the porous media can be considered as a collective process, when the actual combustion wave can be represented by a set of individual flame fronts propagating in mutually connected micro-channels of the different diameter. The discrete structure of the combustion front is most prominent when the inlet velocities are small. In such case, the flame propagation is accomplished with local pulsations which look like downstream/upstream motion within set of channels. These oscillations leads to a irregular propagation of the combustion wave. When the inlet velocities are high enough, the propagation of the flame is free of such processes and looks much more regular. These results suggest that the porous media structure on the scale of the solid grains play an important role in flame propagation. Our model allows to describe the flame anchoring phenomena when the combustion wave is stabilized for a range of inlet velocities, while conventional continuous model predicts the only one value of the inlet velocity for this regime. This result is important because of the possible porous burners application for the domestic and industrial use.

### 3 Acknowledgments

The work was supported financially by the Ministry of education and science of Russian Federation (project 14.Y26.31.0003))

### References

- [1] J.R. Howell, M.J. Hall, J.L. Ellzey (1996). Combustion of hydrocarbon fuels with porous inert media. *Prog. Energy Combust. Sci.* 22: 121.
- [2] L.A. Kennedy, A.A. Fridman, A.V. Saveliev (1996). Superadiabatic combustion in porous media: wave propagation, instabilities, new type of chemical reactor. *J. Fluid Mech. Res.* 22: 1.
- [3] T. Takeno, K. Sato (1979). An excess enthalpy flame theory. *Combust. Sci. Technol.* 20: 73.
- [4] V.S. Babkin, V.I. Drobushевич, Y.M. Laevskii, S.I. Potytnyakov (1983). Filtration combustion of gases. *Combust. Expl. Shock Waves* 19: 147.
- [5] V.S. Babkin, Y.M. Laevskii (1987). Seepage gas combustion. *Combust. Expl. Shock Waves.* 23: 531.
- [6] V.S. Babkin (1993). Filtrational combustion of gases. Present state of affairs and prospects. *Pure Appl. Chem.* 65: 335.
- [7] A.P. Aldushin (1993). New results in the theory of filtration combustion. *Combust. Flame* 94: 308.
- [8] J.F. Liu, W.H. Hsieh (2004). Experimental investigation of combustion in porous heating burners. *Combust. Flame* 138: 295.
- [9] M. Sahraoui, M. Kaviany (1994). Direct simulation vs. volume-averaged treatment of adiabatic, premixed flame in a porous medium. *Int. J. Heat Mass Transfer* 37: 2817.
- [10] P.F. Hsu, R.D. Matthews (1993). The necessity of using detailed chemical kinetics in model for premixed combustion in porous media. *Combust. Flame* 93: 457.
- [11] H.L. Yang, S.S. Minaev, E. Geynce, H. Nakamura, K. Maruta (2009). Filtration combustion of methane in high-porosity micro-fibrous media. *Combust. Sci. Tech.* 181: 1.
- [12] R. Fursenko, S. Minaev, K. Maruta, H. Nakamura, H. Yang (2010). Characteristic regimes of premixed gas combustion in high-porosity micro-fibrous porous media. *Combustion Theory and Modeling* 14: 571.
- [13] K. Maruta, T. Kataoka, N.I. Kim, S. Minaev, R. Fursenko (2005). Characteristics of Combustion in a Narrow channel with a temperature gradient. *Proceedings of the Combustion Institute* 30: 2429.